Li, S., et al., 2020, Mesozoic juvenile crustal formation in the easternmost Tethys: Zircon Hf isotopic evidence from Sumatran granitoids, Indonesia: Geology, v. 48, https://doi.org/10.1130/G47304.1

APPENDIX

Analytical methods

Whole rock geochemical analyses

The samples were crushed after removal of weathered surfaces. The small rock chips were then pulverized into powders using an agate mortar to a grain size of <200 mesh. Whole-rock geochemical analyses were performed at Department of Geosciences, National Taiwan University. Major elements were analyzed by a Rigaku® RIX 2000 X-ray fluorescence (XRF) spectrometer. Loss on ignition (LOI) was analyzed by routine procedures. Trace elements were measured using an Agilent® 7500cx inductively coupled plasma-mass spectrometer (ICP-MS) in the same department. The measurements show a stability range within ~5% variation. Accuracy and precision are generally better than 3%.

Zircon U-Pb analyses

Zircon grains were extracted by heavy liquid and magnetic techniques, and further purified by hand-picking under a binocular microscope. They were set in an epoxy mount which was ground and polished to section the zircons in half. Cathodoluminescence (CL) images were taken using a scanning electron microscope at the Institute of Earth Sciences, Academia Sinica, Taipei, and in order to identify any internal structures and to ensure a selection of good analytical sites.

Zircon U-Pb analyses were performed by the laser ablation-inductively coupled plasma-mass spectrometry (LA-ICP-MS) at Dr. Shen-su Sun Memorial Lab in the Department of Geosciences, National Taiwan University, using a New Wave UP213 laser and an Agilent® 7500s quadrupole ICP-MS. We routinely analyzed standard zircons GJ-1, 91500, and Plešovice to monitor instrumental conditions, yielding weighted mean $^{206}Pb/^{238}U$ ages of 600.4 ± 1.2 Ma

(2σ, N=109), 1060.6 ± 4.2 Ma (2σ, N=28), and 336.6 ± 1.6 Ma (2σ, N=26), respectively, agreement well with the published values (Jackson et al., 2004; Yuan et al., 2004; Sláma et al., 2008). Detailed analytical procedures were described in Chiu et al. (2009, Tectonophysics, v. 477, p. 3-19).

Zircon hafnium isotopic analyses

Zircon Lu-Hf isotopic analyses were performed using a New Wave UP193 laser ablation system attached to a Thermo Finnigan Neptune multi-collector ICP-MS at the Institute of Earth Sciences, Academia Sinica, Taipei. Laser spot diameter was set at 50 μm, with a laser ablation rate of 8 Hz. Standard zircon Mud Tank yielded an average $^{176}Hf/^{177}Hf$ ratio of 0.282493 ± 0.000020 (2σ, N=31), matching well matching with suggested values (Woodhead and Hergt, 2005). Detail Detailed data acquisition and instrumental conditions were same as those reported by Wu et al. (2006, Chemical Geology, v. 234, p. 105-126).

Supplementary figure captions

Figure DR1. Simplified intrusion map of Sumatra, Indonesia (after Barber et al., 2005), showing the main tectonic units, sample locations with zircon U-Pb ages and compiled detrital zircons (Zhang et al., 2019).

Figure DR2. A: Na_2O+K_2O versus SiO_2 diagram for Mesozoic intrusions of Sumatra (Middlemost, 1994). B: Chondrite-normalized rare earth element patterns for Mesozoic intrusions of Sumatra. The values of chondrite and bulk continental crust are from Sun and McDonough (1989), and Rudnick and Gao (2003), respectively. C: Primitive mantle-normalized trace element spider diagrams for Mesozoic intrusions of Sumatra. The values of primitive mantle and bulk continental crust are from Sun and McDonough (1989), and Rudnick and Gao (2003), respectively.

Figure DR3. U-Pb concordia diagrams (A-S) showing zircon ages for Sumatran intrusions obtained by LA-ICPMS.

Figure DR4. Diagram for samples in this study vs. zircon $\varepsilon_{Hf}(t)$ values, showing a marked shift of the zircon Hf array occurring between 205 Ma (sample 14SU35) and 201 Ma (sample 15SU48).

References cited

Andersen, T., 2002, Correction of common lead in U-Pb analyses that do not report 204Pb: Chemical Geology, v. 192, no. 1-2, p. 59-79, doi: 10.1016/S0009-2541(02)00195-X.

Chiu, H.-Y., Chung, S.-L., Wu, F.-Y., Liu, D., Liang, Y.-H., Lin, I. J., Iizuka, Y., Xie, L.-W., Wang, Y., and Chu, M.-F., 2009, Zircon U–Pb and Hf isotopic constraints from eastern Transhimalayan batholiths on the precollisional magmatic and tectonic evolution in southern Tibet: Tectonophysics, v. 477, no. 1, p. 3-19, doi: 10.1016/j.tecto.2009.02.034

Jackson, S. E., Pearson, N. J., Griffin, W. L., and Belousova, E. A., 2004, The application of laser ablation-inductively coupled plasma-mass spectrometry to in situ U–Pb zircon geochronology: Chemical Geology, v. 211, no. 1, p. 47-69, doi: https://doi.org/10.1016/j.chemgeo.2004.06.017.

Middlemost, E. A. K., 1994, Naming materials in the magma/igneous rock system: Earth-Science Reviews, v. 37, no. 3, p. 215-224, doi: 10.1016/0012-8252(94)90029-9.

Sun, S. S., and McDonough, W. F., 1989, Chemical and isotopic systematics of oceanic basalts: implications for mantle composition and processes: Geological Society, London, Special Publications, v. 42, no. 1, p. 313-345, doi: 10.1144/gsl.sp.1989.042.01.19.

Wu, F. Y., Yang, Y. H., Xie, L. W., Yang, J. H., and Xu, P., 2006, Hf isotopic compositions of the standard zircons and baddeleyites used in U-Pb geochronology: Chemical Geology, v. 234, no. 1-2, p. 105-126, doi: 10.1016/j.chemgeo.2006.05.003.

Zhang, X., Chung, S.L., Lai, Y.M., Ghani, A. A., Murtadha, S., Lee, H.Y., and Hsu, C.C., 2019, A 6000-km-long Neo-Tethyan arc system with coherent magmatic flare-ups and lulls in South Asia: Geology, v. 47, no. 6, p. 573-576, doi: https://doi.org/10.1130 /G46172.1.

Yuan, H., Gao, S., Liu, X., Li, H., Günther, D., and Wu, F., 2004, Accurate U-Pb Age and Trace Element Determinations of Zircon by Laser Ablation-Inductively Coupled Plasma-Mass Spectrometry: Geostandards and Geoanalytical Research, v. 28, no. 3, p. 353-370, doi: 10.1111/j.1751-908X.2004.tb00755.x.

Sláma, J., Košler, J., Condon, D. J., Crowley, J. L., Gerdes, A., Hanchar, J. M., Horstwood, M. S. A., Morris, G. A., Nasdala, L., Norberg, N., Schaltegger, U., Schoene, B., Tubrett, M. N., and Whitehouse, M. J., 2008, Plešovice zircon — A new natural reference material for U–Pb and Hf isotopic microanalysis: Chemical Geology, v. 249, no. 1–2, p. 1-35.

Woodhead, J. D., and Hergt, J. M., 2005, A Preliminary Appraisal of Seven Natural Zircon Reference Materials for In Situ Hf Isotope Determination: Geostandards and Geoanalytical Research, v. 29, no. 2, p. 183-195, doi: 10.1111/j.1751-908X.2005.tb00891.x.

Barber, A. J., Crow, M. J., and Milsom, J. S., 2005, Sumatra: Geology, Resources and Tectonic Evolution, London, Geological Society, London, Memoirs, v. 31.

Rudnick, R. L., and Gao, S., 2003, 3.01 - Composition of the Continental Crust, in Turekian, H. D. H. K., ed., Treatise on Geochemistry: Oxford, Pergamon, p. 1-64.

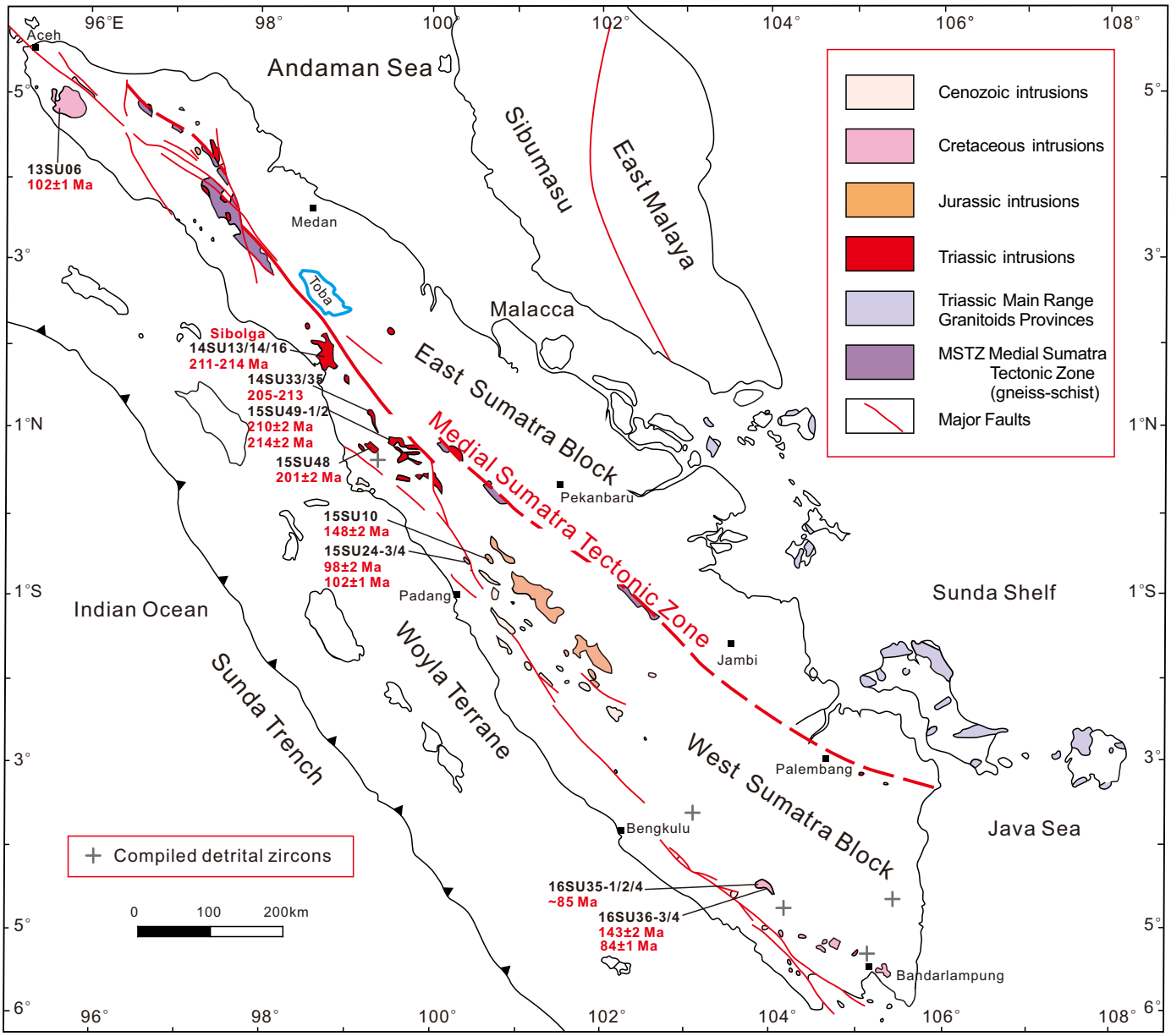

Figure DR1. Simplified intrusion map of Sumatra, Indonesia (after Barber et al., 2005), showing the main tectonic units, sample locations with zircon U-Pb ages and compiled detrital zircons (Zhang et al., 2019).

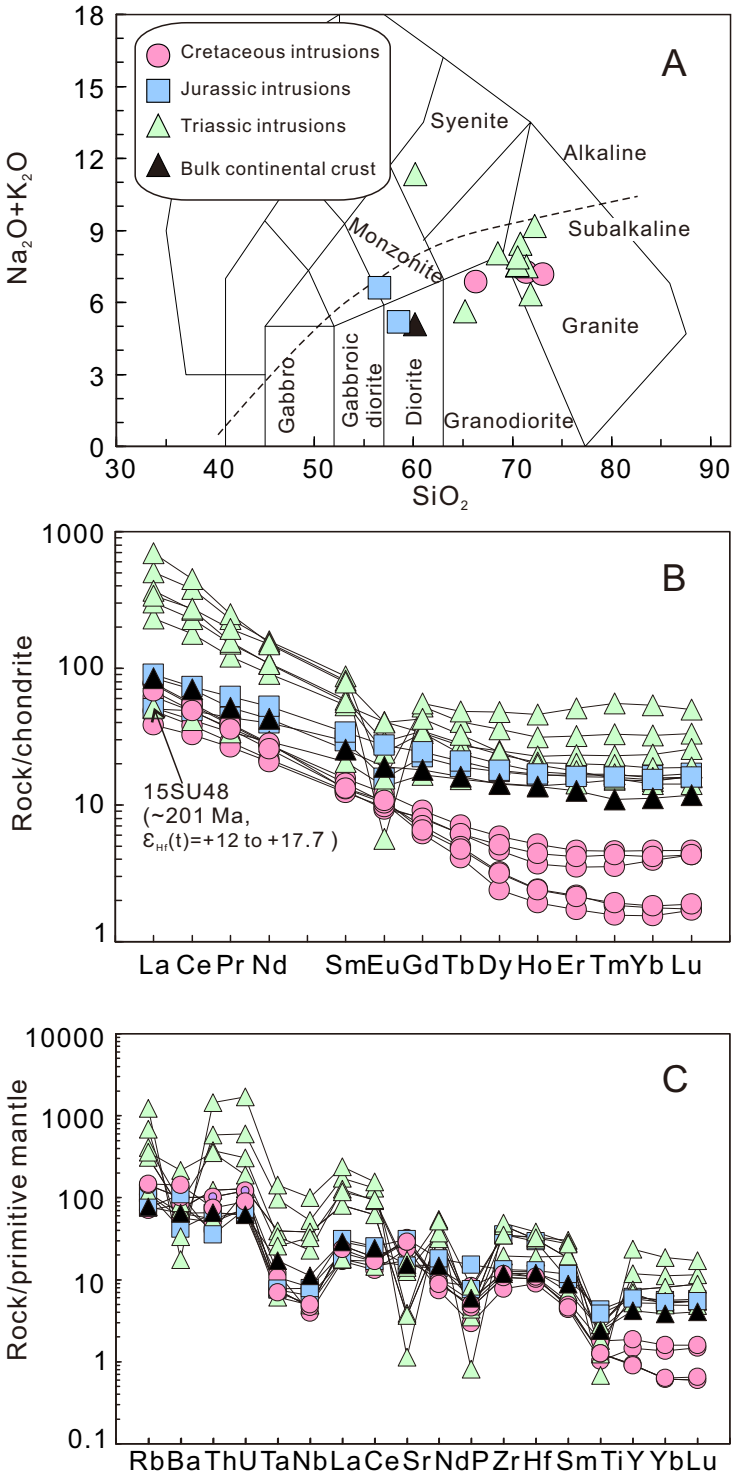

Figure DR2. A: Na2O+K2O versus SiO2 diagram for Mesozoic intrusions of Sumatra (Middlemost, 1994). B: Chondrite-normalized rare earth element patterns for Mesozoic intrusions of Sumatra. The values of chondrite and bulk continental crust are from Sun and McDonough (1989), and Rudnick and Gao (2003), respectively. C: Primitive mantle-normalized trace element spider diagrams for Mesozoic intrusions of Sumatra. The values of primitive mantle and bulk continental crust are from Sun and McDonough (1989), and Rudnick and Gao (2003), respectively.

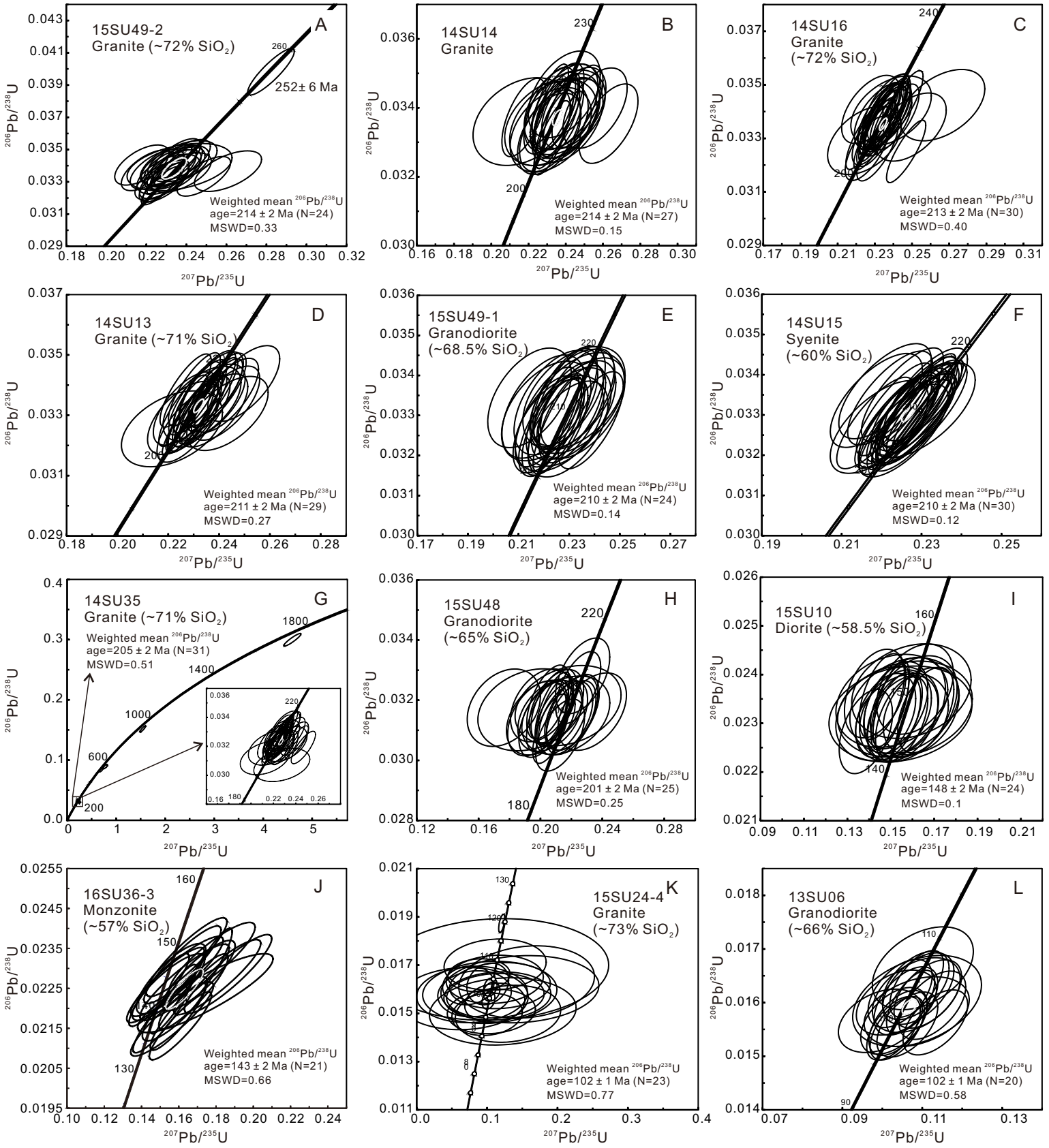
A
15SU49-2
Granite (~72% SiO2)
252± 6 Ma
Weighted mean 206Pb/238U
age=214 ± 2 Ma (N=24)
MSWD=0.33
B
14SU14
Granite
Weighted mean 206Pb/238U
age=214 ± 2 Ma (N=27)
MSWD=0.15
C
14SU16
Granite
(~72% SiO2)
Weighted mean 206Pb/238U
age=213 ± 2 Ma (N=30)
MSWD=0.40
D
14SU13
Granite (~71% SiO2)
Weighted mean 206Pb/238U
age=211 ± 2 Ma (N=29)
MSWD=0.27
E
15SU49-1
Granodiorite
(~68.5% SiO2)
Weighted mean 206Pb/238U
age=210 ± 2 Ma (N=24)
MSWD=0.14
F
14SU15
Syenite
(~60% SiO2)
Weighted mean 206Pb/238U
age=210 ± 2 Ma (N=30)
MSWD=0.12
G
14SU35
Granite (~71% SiO2)
Weighted mean 206Pb/238U
age=205 ± 2 Ma (N=31)
MSWD=0.51
H
15SU48
Granodiorite
(~65% SiO2)
Weighted mean 206Pb/238U
age=201 ± 2 Ma (N=25)
MSWD=0.25
I
15SU10
Diorite (~58.5% SiO2)
Weighted mean 206Pb/238U
age=148 ± 2 Ma (N=24)
MSWD=0.1
J
16SU36-3
Monzonite
(~57% SiO2)
Weighted mean 206Pb/238U
age=143 ± 2 Ma (N=21)
MSWD=0.66
K
15SU24-4
Granite
(~73% SiO2)
Weighted mean 206Pb/238U
age=102 ± 1 Ma (N=23)
MSWD=0.77
L
13SU06
Granodiorite
(~66% SiO2)
Weighted mean 206Pb/238U
age=102 ± 1 Ma (N=20)
MSWD=0.58
206Pb/238U
207Pb/235U

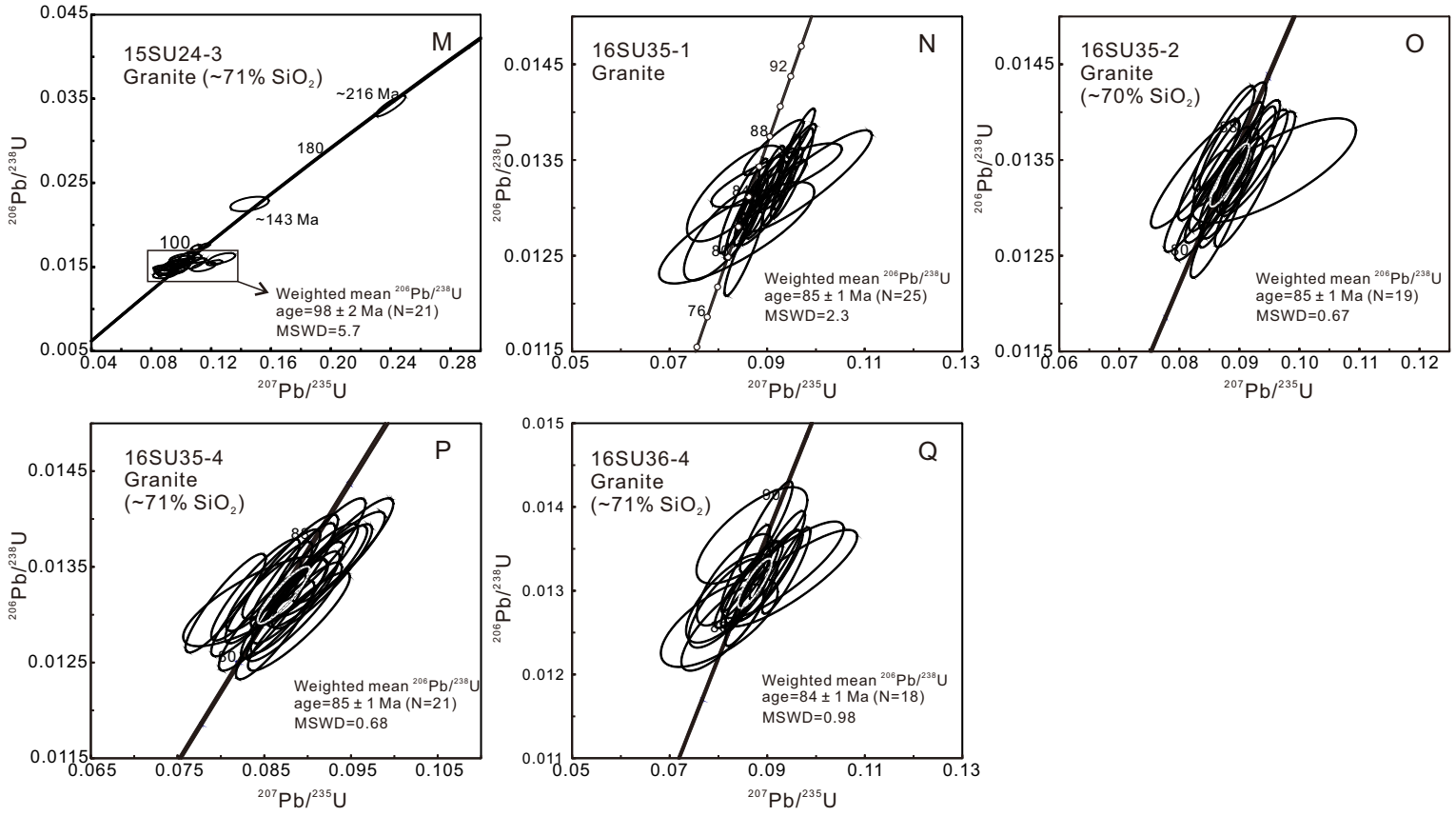

Figure DR3. U-Pb concordia diagrams (A-S) showing zircon ages for Sumatran intrusions obtained by LA-ICPMS.

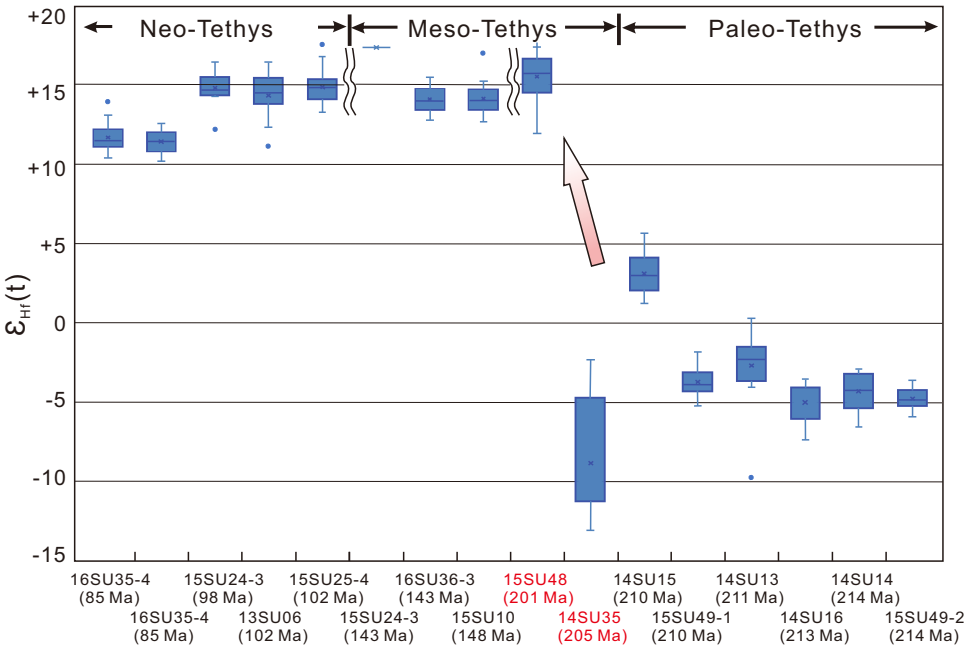

Figure DR4. Diagram for samples in this study vs. zircon εHf(t) values, showing a marked shift of the zircon Hf array occurring between 205 Ma (sample 14SU35) and 201 Ma (sample 15SU48).